Tomography of the Galactic Center region with imaging X-ray polarimetry
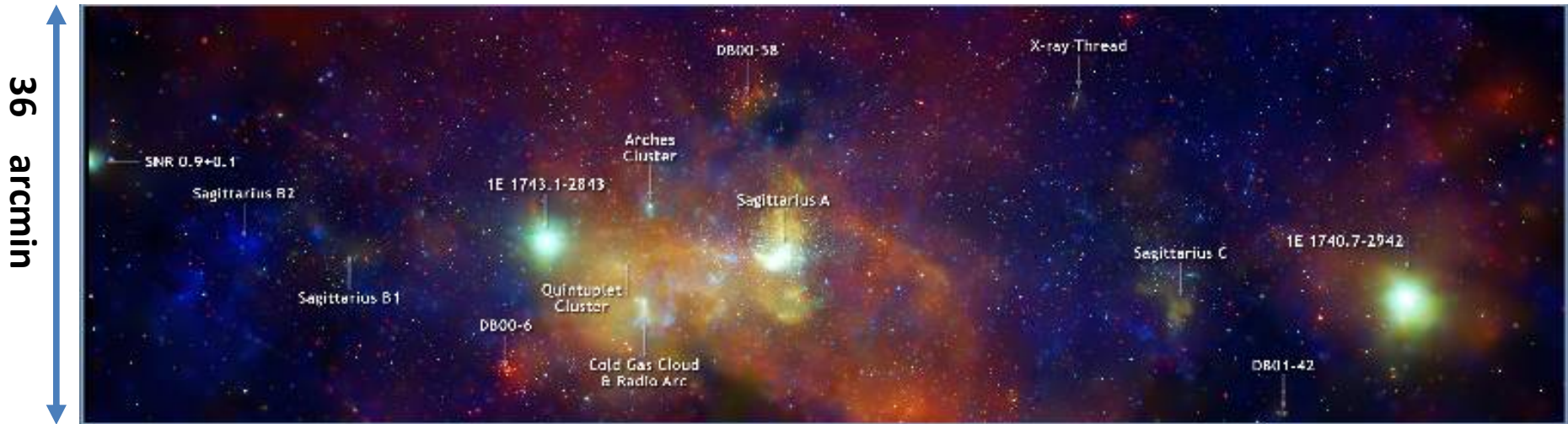
Paolo Soffitta

IAPS/INAF (Rome, Italy)

Frédéric Marin, Fabio Muleri,Vladimir Karas, Devaky Kunneriath
on behalf of IXPE and XIPE teams

900 x 400 Ly of the Galactic Center as seen in X-rays by Chandra

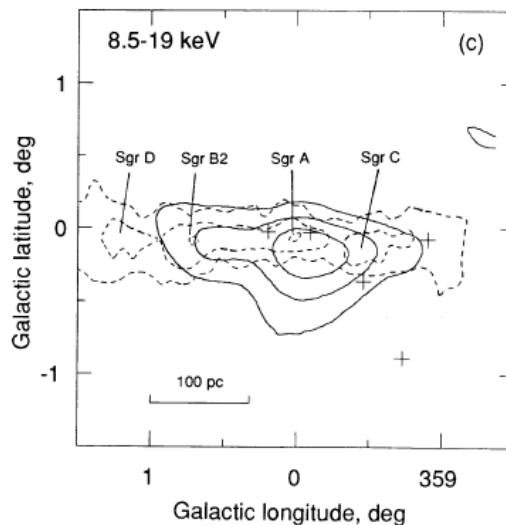**117 arcmin;** color code : **1-3 keV ; 3-5 keV; 5-8 keV**

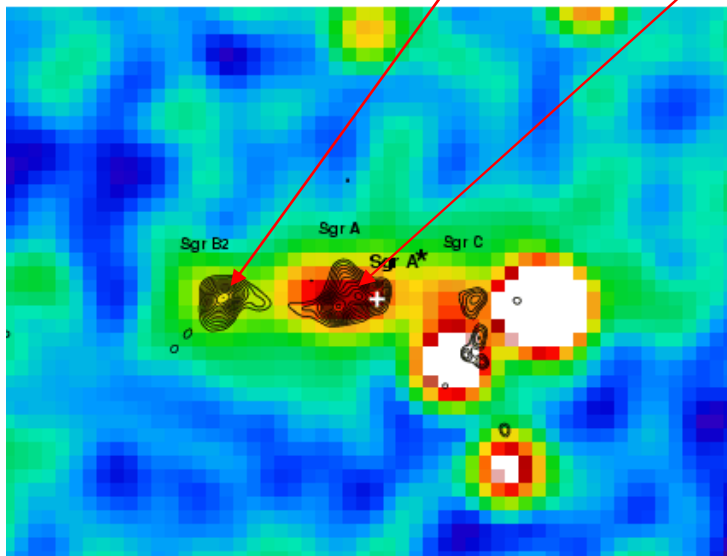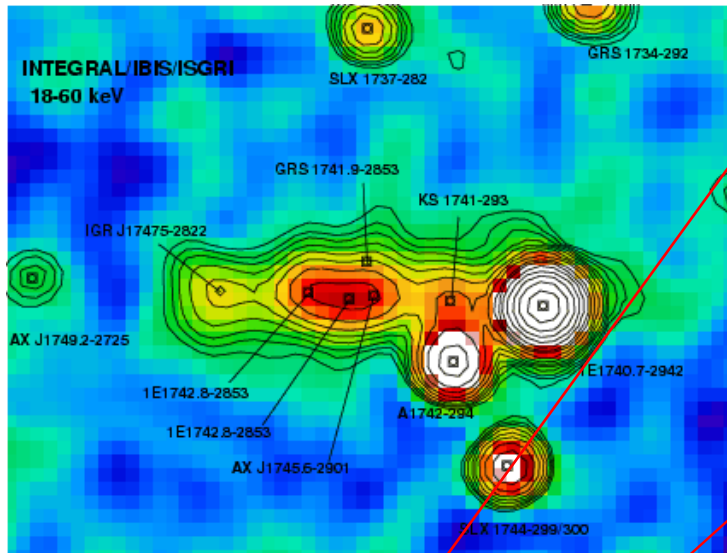**Center Nebular Zone**

Sunyaev et al., 1993

Art-P on GRANAT

Sunyaev et al., suggested that part of the emission in the galactic center region could be due to Thomson scattering by dense molecular clouds.
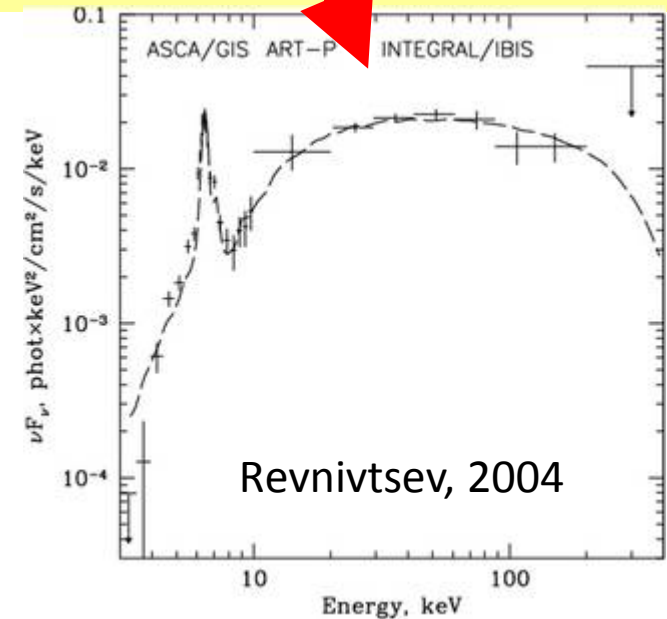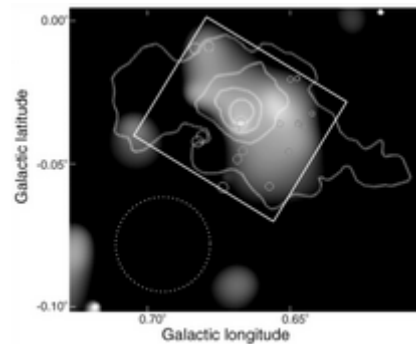
Sgr B Complex

Sgr C Complex

Sgr A Complex

The strange case of Sgr B2

SgrB2 is a giant molecular cloud at ~100pc projected distance from the Black Hole

The spectrum of SgrB2 is a pure reflection spectrum (Sunyaev et al. 1993)

But no bright enough source is there !!!

Revnivtsev, 2004

The emission from SgrB2 is extended and brighter in the direction of the BH (Murakami 2001). It is also varying in time (Inui et al. 2008).

Is SgrB2 echoing past emission from the BH, which was therefore one million time more active ~300 years ago ??? (e.g. Koyama et al. 1996)

INTEGRAL Image of GC (Revnivtsev 2004)

3

Was the GC an AGN a few hundreds years ago?

X-ray polarimetry can definitively proof or reject this hypothesis.

<u>SgrB2 should be highly polarized with the electric vector perpendicular to the line connecting the two sources.</u>
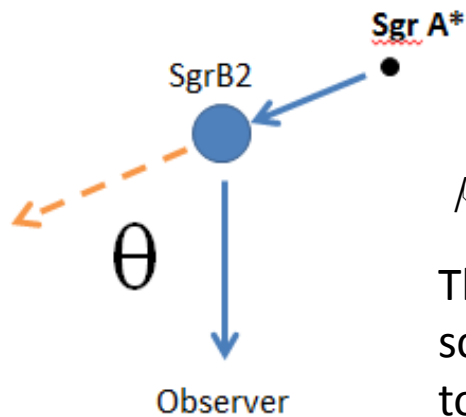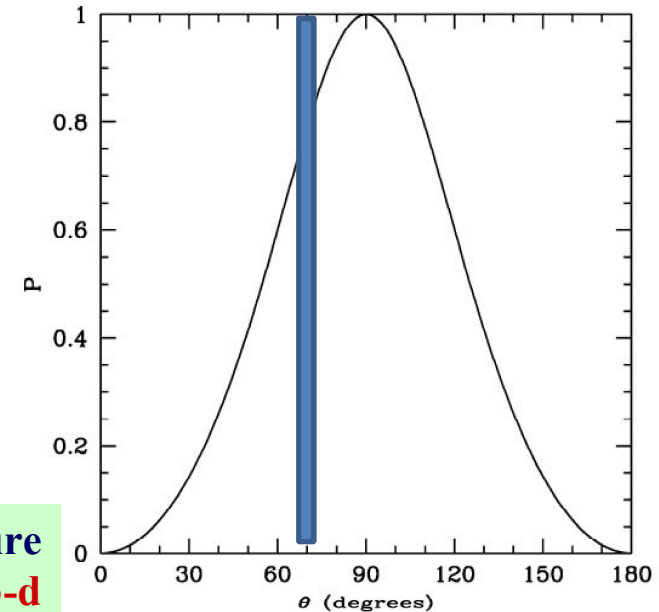

$$P = \frac{1 - \mu^2}{1 + \mu^2}$$

$$\mu = \cos(\vartheta)$$

The polarization direction of the scattered radiation is **perpendicular** to the scattering plane.

The degree of polarization would measure the angle and provide a full 3-d representation of the clouds (Churazov et al. 2002)

$$L_8 \approx 6 10^{38} \times \left(\frac{F_{6.4}}{10^{-4}}\right) \times \left(\frac{0.1}{\tau_T}\right) \times \left(\frac{\delta_{Fe}}{3.3 \times 10^{-5}}\right)^{-1}$$
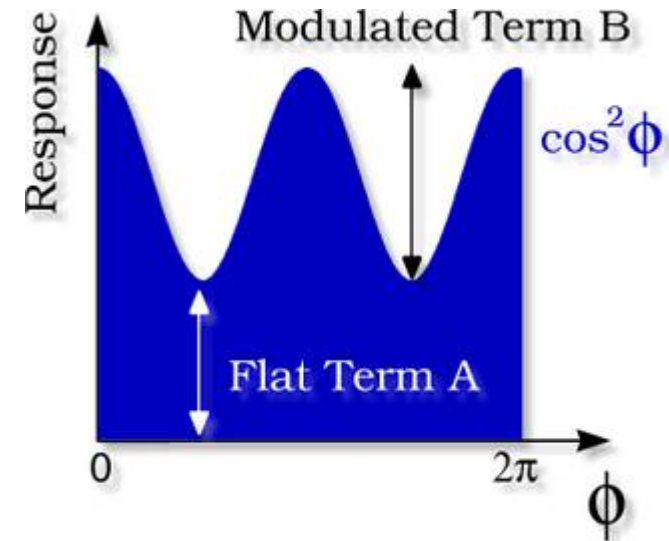$$\times \left(\frac{R}{100 \text{ pc}}\right)^2$$

From the distance to the source is possible to derive its luminosity at a given epoch

X-ray polarimetry: fundamental parameters

Fit function: $\mathcal{M}(\phi) = A + B\cos^2(\phi - \phi_0)$

ϕ is the azimuthal angle, that is the angle with respect to the electric vector of the 'carrier' of the polarization information

Modulation: $\dfrac{\mathcal{M}_{\max} - \mathcal{M}_{\min}}{\mathcal{M}_{\max} + \mathcal{M}_{\min}}$ $\dfrac{B}{B + 2A}$

Modulation factor, μ : the modulation for 100% linearly polarized radiation is the key parameter of a polarimeter and ranges between 0 (no polarimetric sensitivity) to 1 (maximum sensitivity to polarization).

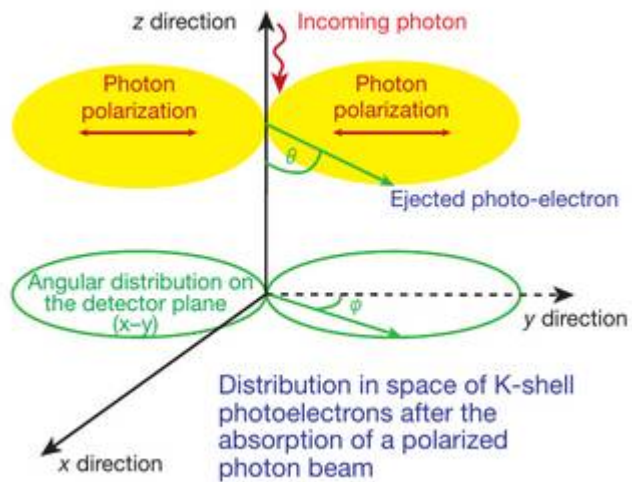Degree of Polarization is the modulation divided by the modulation factor.

$P = \dfrac{1}{\mu}\dfrac{B}{B + 2A}$

Congresso Nazionale della SIF.
Sezione Astrofisica

The Gas Pixel Detector

We developed at this aim a polarization-sensitive instrument capable of imaging, timing and spectroscopy
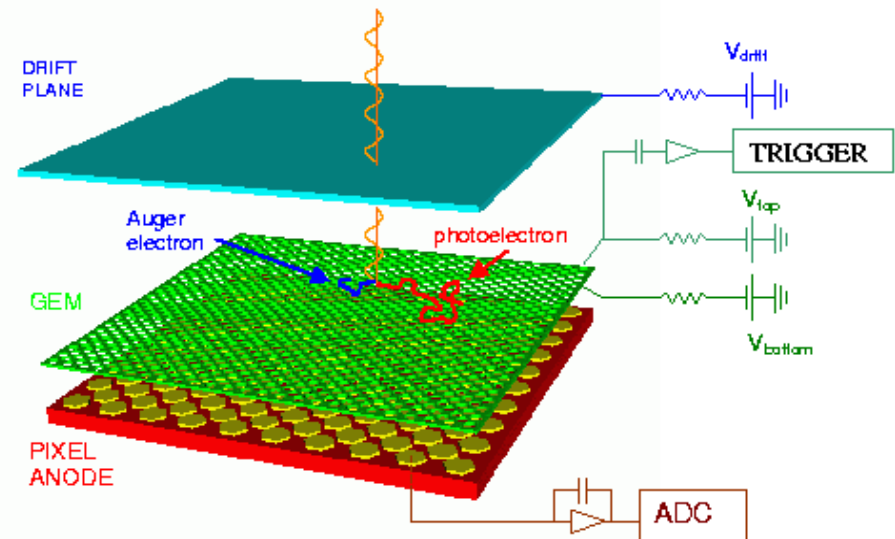
The photoelectric effect

The Gas Pixel Detector

$$\frac{\partial \sigma}{\partial \Omega} = r_0^2 \frac{Z^5}{137^4} \left(\frac{mc^2}{h\nu}\right)^{7/2} \frac{4\sqrt{2}\sin^2(\theta)\cos^2(\varphi)}{(1 - \beta\cos(\theta))^4}$$


z direction — Incoming photon

Photon polarization — Photon polarization

θ

Ejected photo-electron

Angular distribution on the detector plane (x–y)

φ

y direction

Distribution in space of K-shell photoelectrons after the absorption of a polarized photon beam

x direction

E. Costa et al. 2001, Bellazzini et al., 2006, 2007

DRIFT PLANE

V_{drift}

TRIGGER

V_{top}

Auger electron

photoelectron

GEM

V_{bottom}

PIXEL ANODE

ADC

GPD

Flexible cables
Ti frame
Be window
Gas cell
GEM
Miniboard
Al flange

Laboratory DAQ

The direction of the ejected photoelectron is statistically related to the polarisation of the absorbed photon.
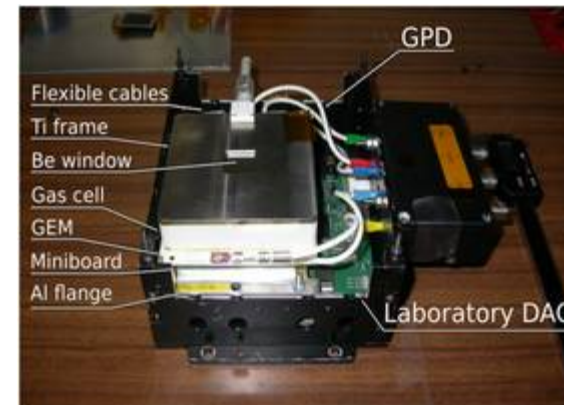
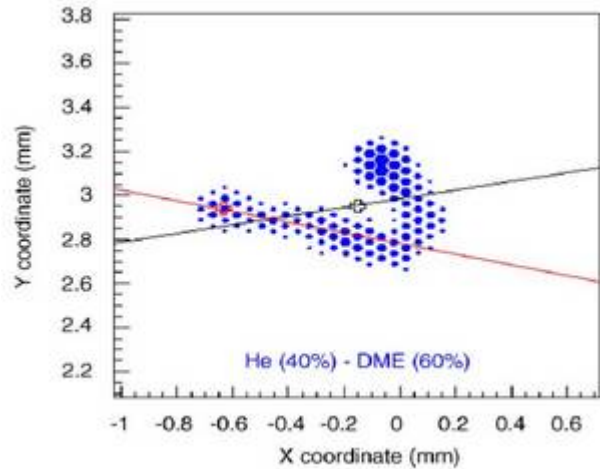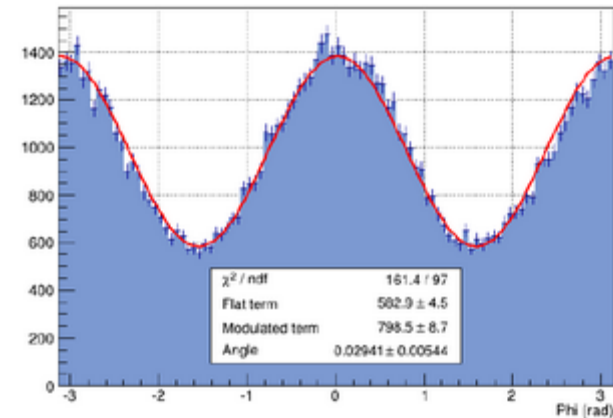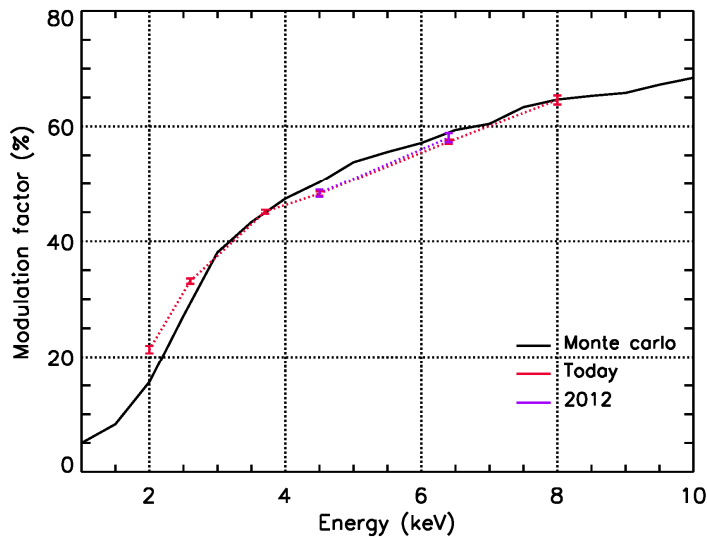# The Gas Pixel Detector: Polarimetry capability

Image of a real photoelectron track. The use of the gas allows to resolve tracks in the X-ray energy band.
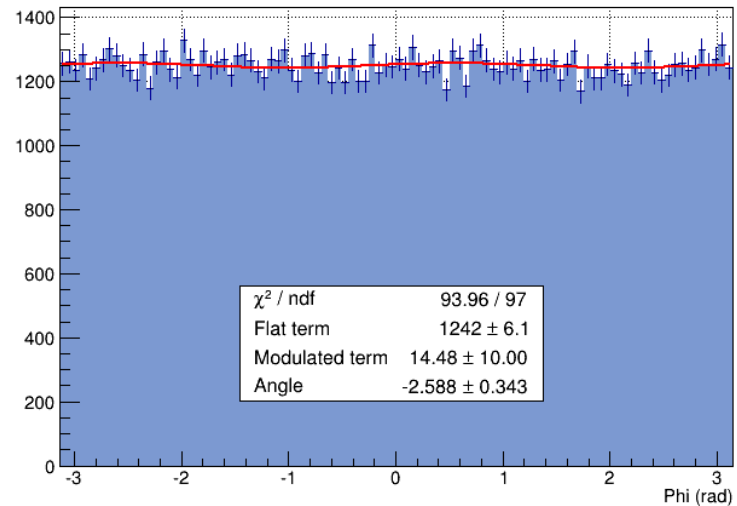

Real modulation curve derived from the measurement of the emission direction of the photoelectron.

Muleri et al. 2008,2010

Modulation factor as a function of energy.


Bellazzini et al. 2012

Residual modulation for unpolarised photons.

The Gas Pixel Detector: imaging capability

- Good spatial resolution: 90 μm Half Energy Width

- Imaging capabilities on- and off-axis measured at PANTER with a JET-X telescope (Fabiani et al. 2014)

- Angular resolution for Jet-X optics (23.2'' at 4.5 keV) (XIPE optics : <26 arcsec).

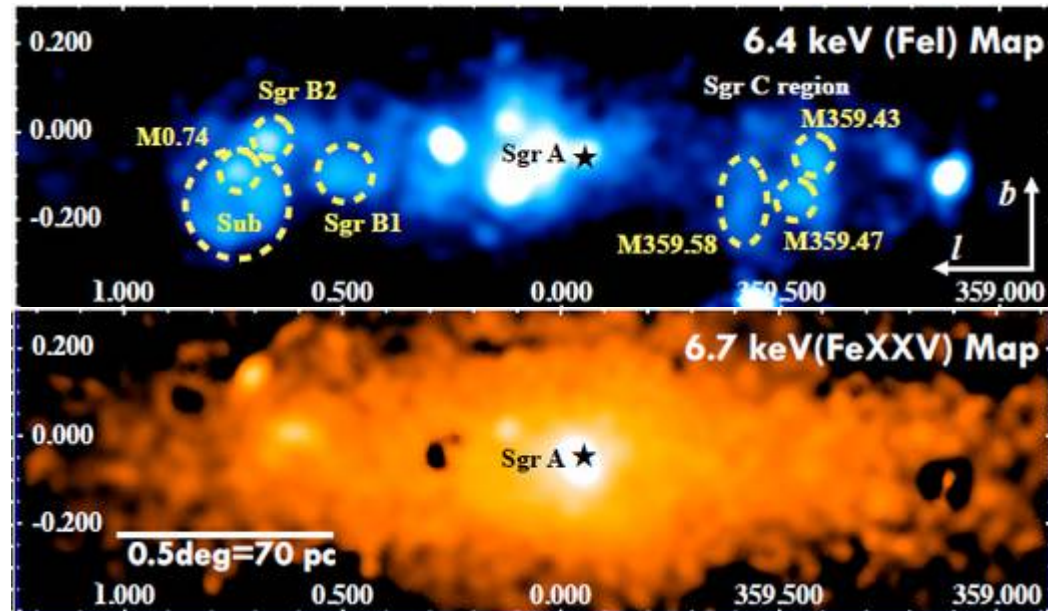Off axis PSF Impact Point Map at 2.98 keV
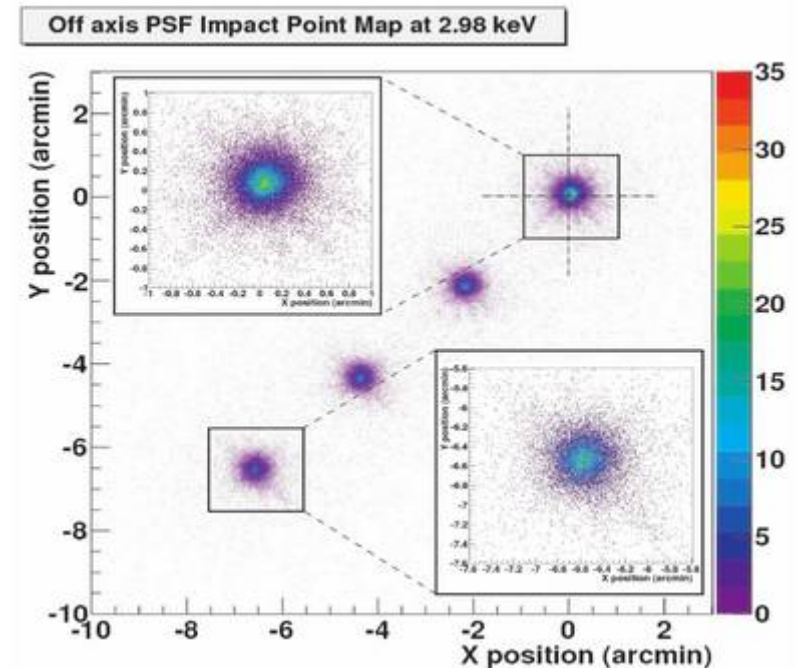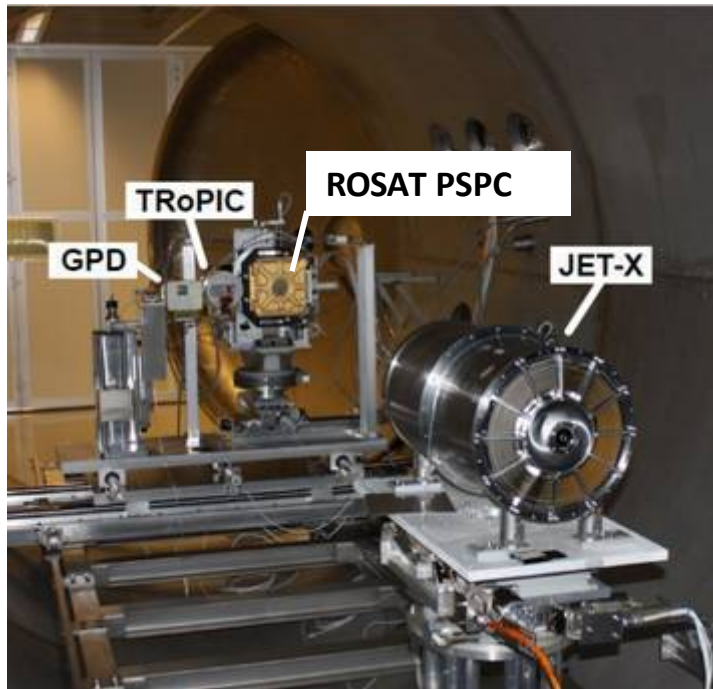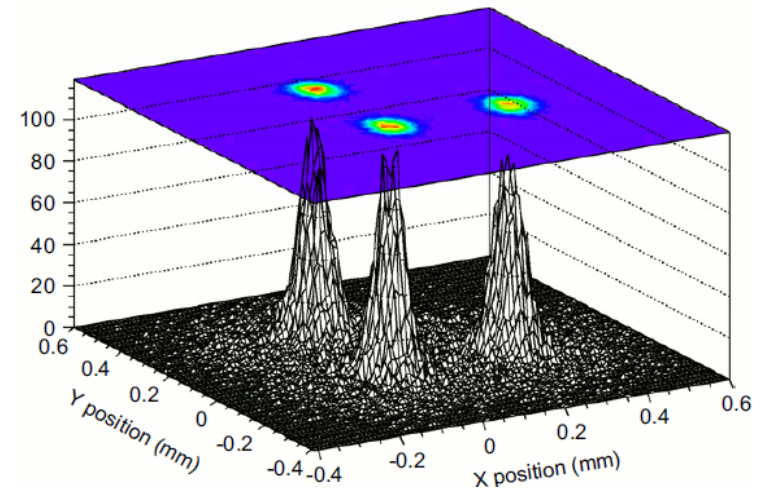
The gas pixel detector: spectroscopic capabilities
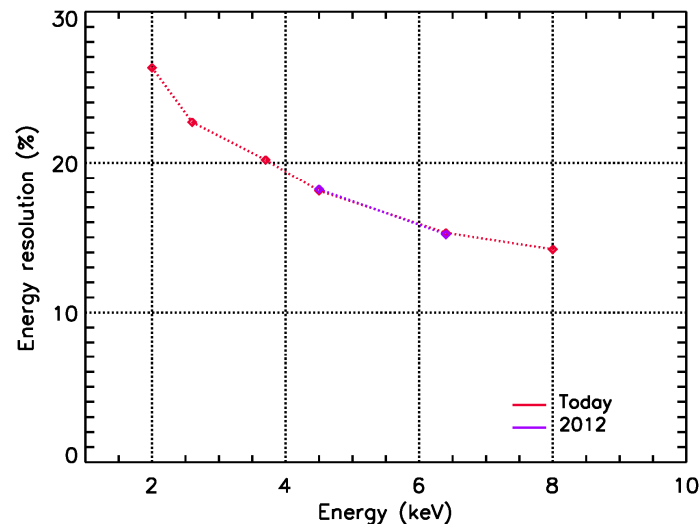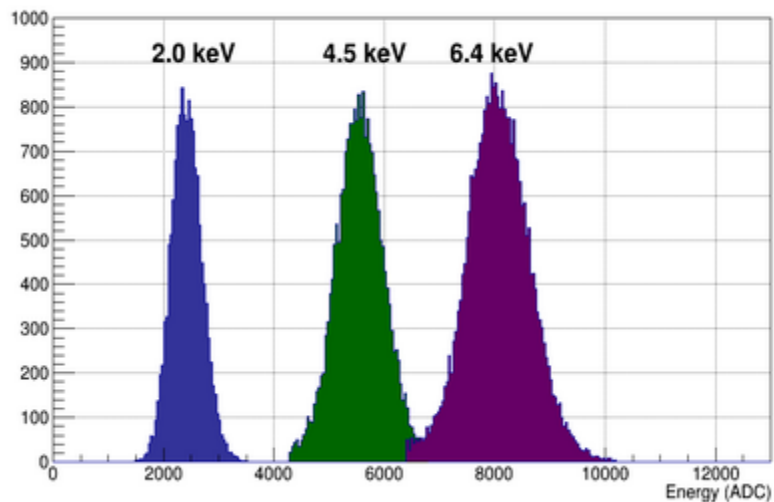
- Adequate spectrometer for continuum emission (16 % at 6 keV, Muleri et al. 2010).

- Stable operation over 3 years

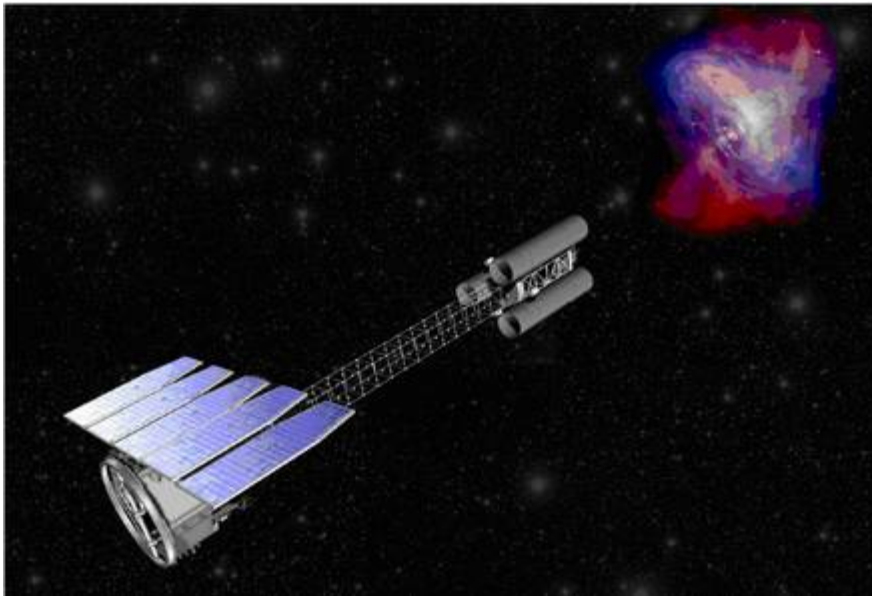Congresso Nazionale della SIF.
Sezione Astrofisica
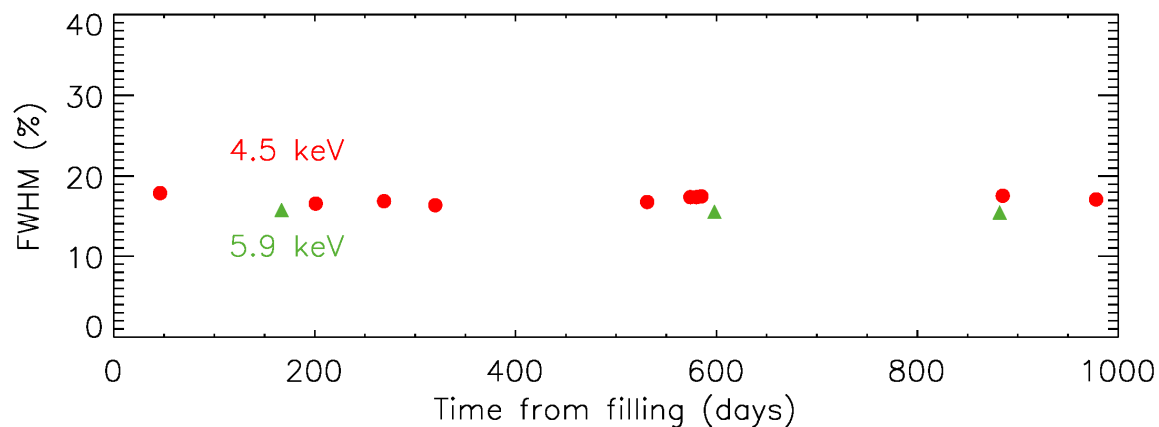
X-ray polarimetry < 10 keV it is not so easy.

Suzaku X-ray map of X-ray Reflection Nebulae (top), hot plasma (right) in GC by Suzaku/XIS
(Ryu et al., 2012)

- A diffuse emission typical of a hot plasma (6.5 keV) is present in the Galactic center region providing not polarized component.
- The expected polarization due to reflection must be diluted considering this contribution.

Two proposed missions: IXPE and XIPE

IXPE (Imaging X-ray Polarimetry Explorer, PI M. Weisskopf MSFC) NASA Small Explorer (**selected for Phase A with other 2 missions**)

XIPE (X-ray Imaging Polarimetry Explorer) ESA M4 mission (**selected for Study Phase with other 2 missions**).

Payload of IXPE and XIPE: three GPDs (2-8 keV) coupled to three conventional X-ray optics.

XIPE design guidelines

- Three telescopes with 3.5 m focal length to fit within the Vega fairing.
    Long heritage: SAX → XMM → Swift → eROSITA → XIPE
- Pioneering, yet mature detectors: conventional proportional counter but with a revolutionary readout.
- Mild mission requirements: 1 mm alignment, 1 arcmin pointing.
- Fixed solar panel. No deployable structure. No cryogenics. No movable part except for the filter wheels.
- Low payload mass: 265 kg with margins. Low power consumption: 129 W with margins.
- Three years of nominal operation. No consumables.
- Low Earth equatorial orbit.
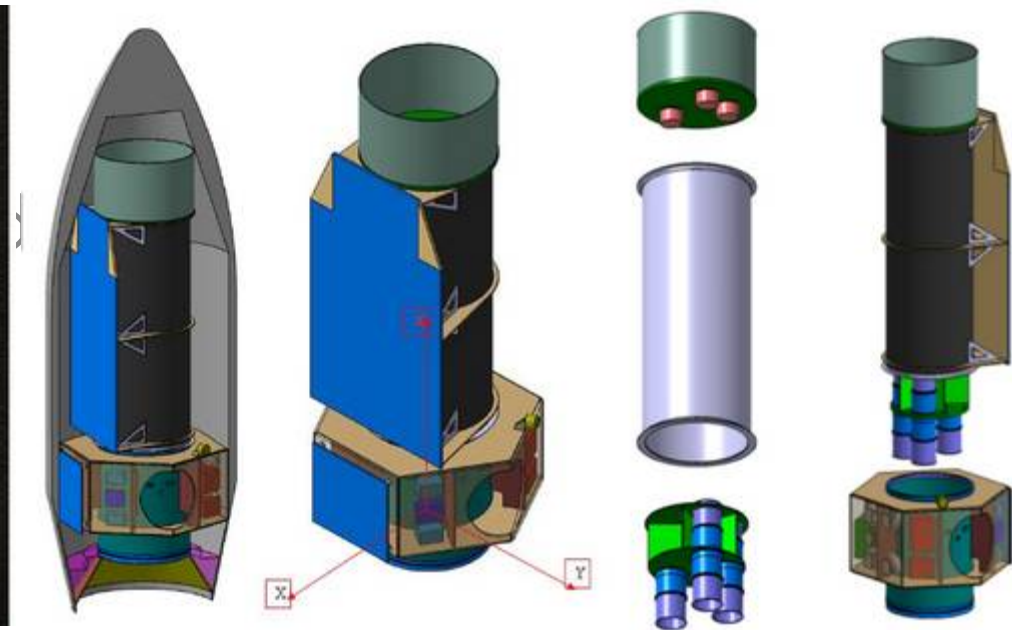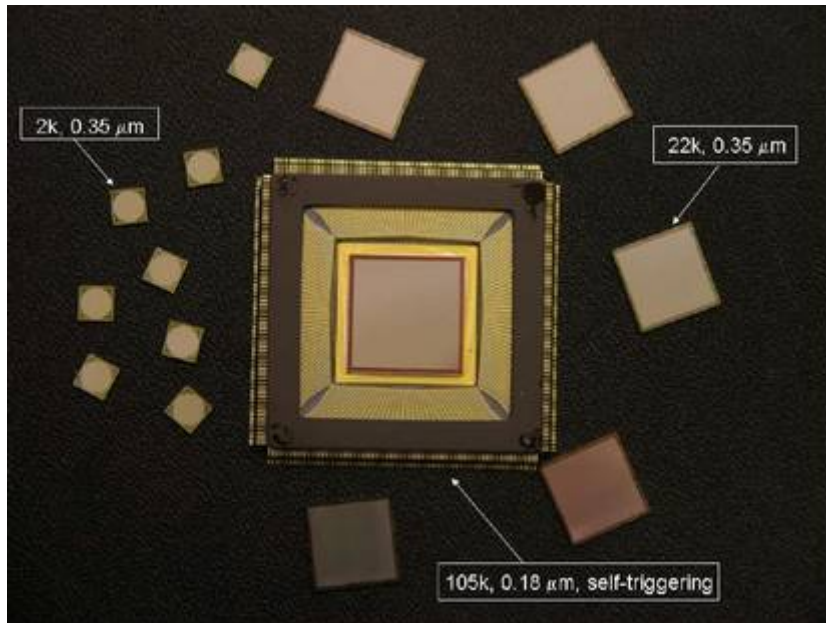
Bellazzini et al. 2006, 2007

Congresso Nazionale della SIF.
Sezione Astrofisica

4 keV <E < 8 keV
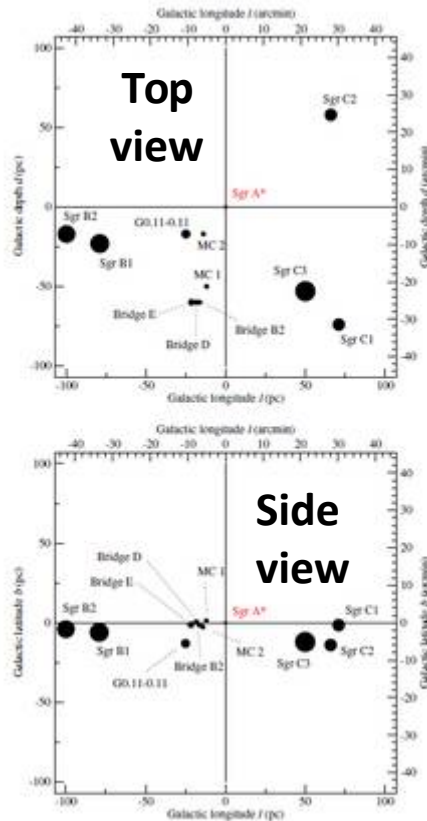
Sketch of the GC model as seen from two directions.
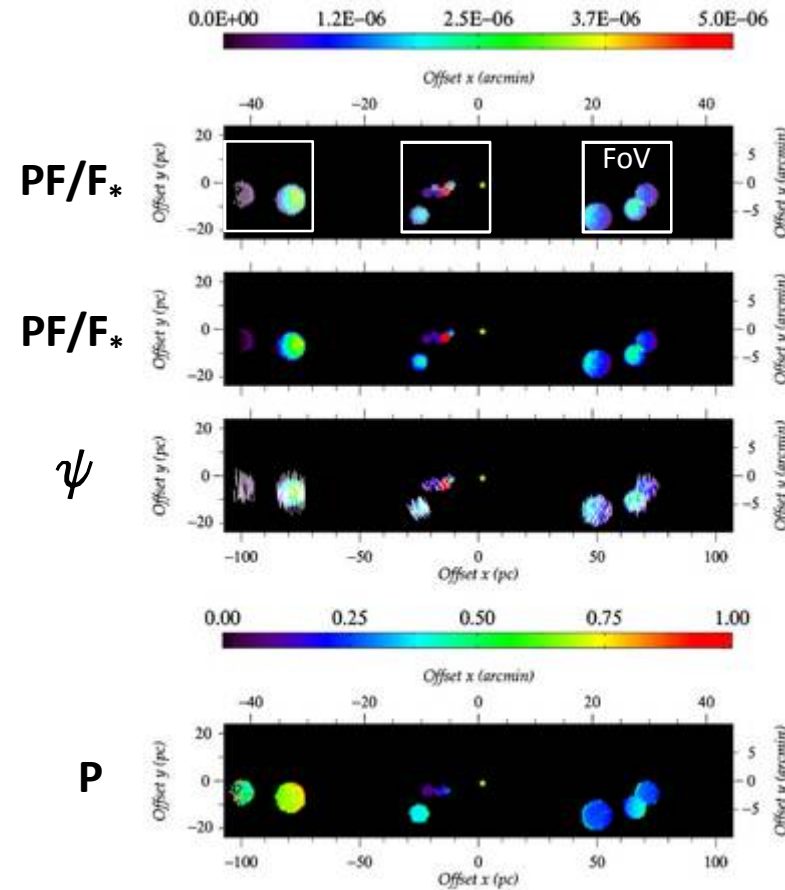
Marin et al., 2015

Three-dimensional radiative transfer is achieved by using STOKES Monte Carlo code: polarization treatment, multiple scattering , and an imaging routine.

Sgr A* flares are too faint with a small duration (MDP= 28 % integrating on 4 Ms)

E = 4-8 keV
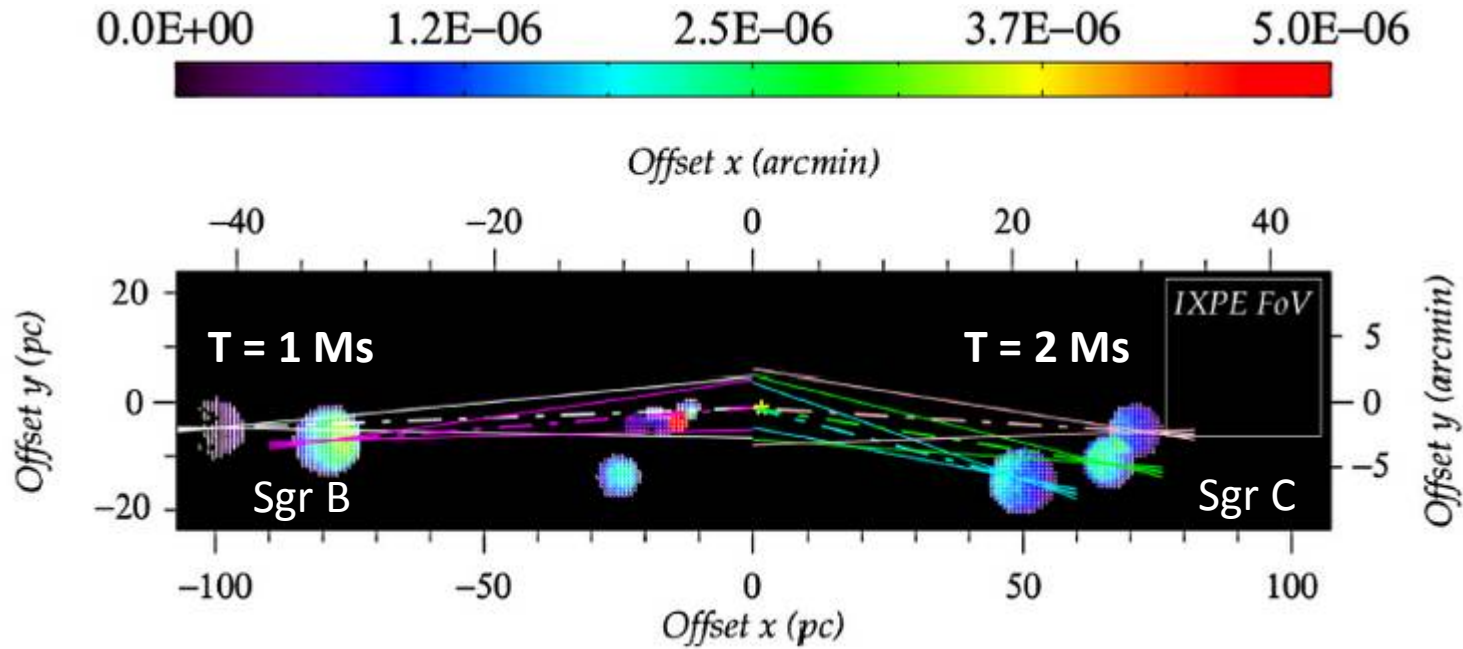
Molecular cloud	P (%)	ψ (°)	f_R (%)	$P_{exp.}$ (%)	$P_{detect.}$ (%)	$\psi_{detect.}$ (°)
Sgr B2	65.0	88.3	70.0	45.5	57.4 ± 4.4	83.3 ± 3.4
Sgr B1	76.9	84.4	52.6	40.5	40.4 ± 3.9	80.3 ± 3.3
G0.11-0.11	55.8	61.6	–	–	–	–
Bridge E	12.7	67.9	–	–	–	–
Bridge D	0.1	74.2	–	–	–	–
Bridge B2	15.8	77.8	–	–	–	–
MC2	25.8	73.8	–	–	–	–
MC1	0.1	77.5	–	–	–	–
Sgr C3	32.9	106.4	50.7	16.7	15.5 ± 2.4	109.0 ± 4.5
Sgr C2	34.9	99.1	63.0	22.0	17.9 ± 3.8	99.1 ± 5.6
Sgr C1	31.1	94.6	60.2	18.7	23.1 ± 3.3	98.1 ± 6.0

Molecular clouds are brighter on the side of SgrA* (as observed for SgrB2).

G0.11-0.11, the Bridge, MC1, or MC2 are observable with a single pointing. A lower net polarization and an increased contribution of the plasma emission is expected. The results for Sgr B and Sgr C complex will drive their observation.

Marin et al., 2015

Conclusions

- X-ray polarimetry with the Gas Pixel Detector at the focus of an X-ray optics pinpoints the eventual illuminating source of the molecular nebulae by measuring the polarization angle. It is a viable tool to proof if SgA* is this source.

- X-ray polarimetry can fix, with the measure of the degree of polarization, the true distance of the reflecting nebulae to Sgr A* helping defining the correct light-curve of its flare.

- Measurement is possible with XIPE and IXPE in 4 keV < E < 8 keV energy band at least for Sgr B and Sgr C complex by taking care of the Galactic Center Plasma emission that dilute the polarization degree due to scattering.

- Alternative hypothesis (e.g. cosmic rays interaction with molecular clouds) can be ruled out.

Suzaku view of Sgr B2 emission

(Ryu 2009)

(Ryu, 2013)
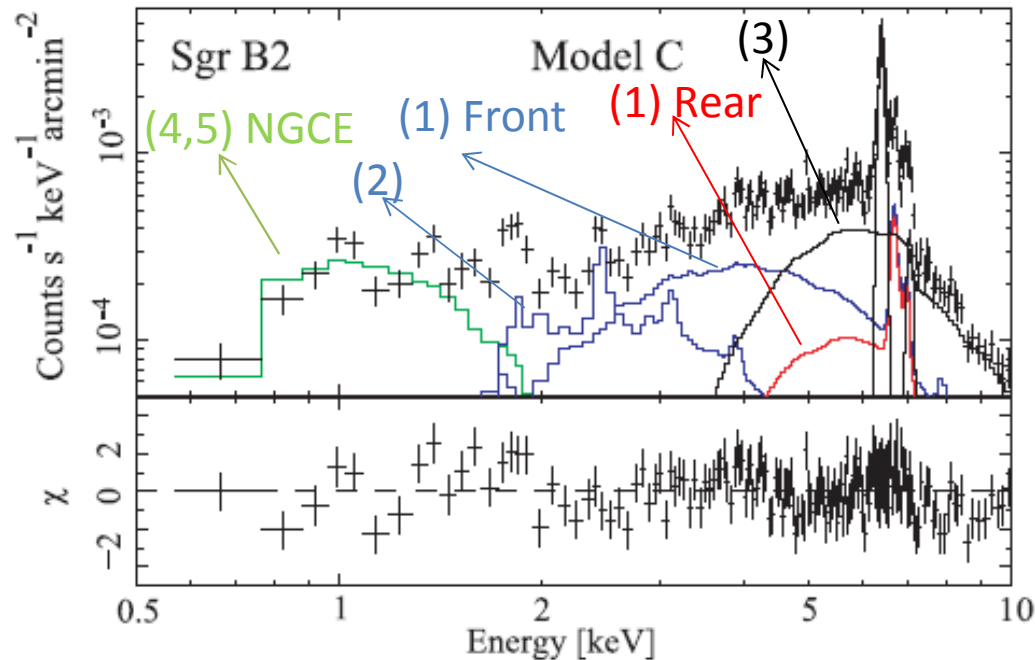
NGCE Non Galactic center emission

(1) Very hot plasma responsible for the 6.7 keV-line.
(2) Hot plasma responsible for the 2.45 keV-line.
(3) Cool gas component that emits the 6.4 keV-line.
(4) Low energy (0.5–2 keV) X-rays with small absorption.
(5) The cosmic X-ray background (CXB).

Position of Sgr B2 along the line of sight.
Best fit of Sgr B2 spectrum embedded in hot plasma (Ryu 2009).

Sgr C is a complex of three sources distant from each others (Ryu, et al, 2013).

Large number of counts needed

Minimum Detectable Polarization (99%): $$MDP = \frac{4.29}{\mu \times S} \times \sqrt{\frac{S+B}{T}}$$

S is the source rate, B is the background rate, T is the observing time, μ is the modulation factor.

If background is negligible like is the case for focal plane X-ray polarimeters

$$MMM = \frac{4.29}{\sqrt{MMMMM}}$$

To reach MDP=1% with μ=0.5:

$$Counts = \left(\frac{4.29}{\mu\,MDP}\right)^2 \qquad = 736\ 10^3\ \text{Counts}$$

Source **detection**:   >   10 counts
Source **spectrum slope**: > 100 counts
Source **polarimetry**:   > 100,000 counts

Table 1. Parameterization of the reflection nebulae, modeled with uniform-density, spherical clouds filled with cold, solar abundance matter.

Molecular cloud	Cloud radius (pc)	Projected distance[a] (pc)	Line of sight distance[b] (pc)	Offset[c] (pc)	Velocity[d] (km s^{-1})	Hydrogen column density ($\times 10^{22}$ cm^{-2})	Electron optical depth	References
Sgr B2	5	−100	−17	−4.0	60	80	0.5	E, I
Sgr B1	6	−79.1	−23	−6	−45	12.3	0.3	A, D, G
G0.11-0.11	3.7	−25	−17	−13	25	2	0.03	E, F
Bridge E	2.0	−21.6	−60	−1.3	55	9.6	0.07	B, E, F
Bridge D	1.6	−18.3	−60	0.5	55	13.2	0.09	B, E, F
Bridge B2	1.8	−16.3	−60	−1.5	55	12.3	0.08	B, E, F
MC2	1.8	−14	<−17	−2.6	−10	<2	0.36	C, E
MC1	1.8	−12	−50	1.3	−15	4	0.32	E
Sgr C3	6	50	−53	−12	60	8.7	<1	H, E
Sgr C2	4.7	66	58	−14	60	11.4	<1	H, E
Sgr C1	4.7	71	−74	−1.5	60	6.5	<1	H, E

Notes. [a] Positive = east of the Galactic center; [b] Positive = behind the Galactic plane (farther to us than Sgr A*); [c] Positive = above the equatorial plane. [d] Positive = away from Earth.

References. A: An et al. (2013); B: Capelli et al. (2012); C: Clavel et al. (2013); D: Downes et al. (1980); E: Ponti et al. (2010); F: Ponti et al. (2014); G: Ryu et al. (2009); H: Ryu et al. (2013) and I: Sunyaev et al. (1993).

Using time and spectroscopy to study of Sgr A complex

Region from Sgr A* and the radio arc

Studies with XMM and Chandra revealed the presence of molecular clouds (MC) possibly reflecting and reprocessing radiation from Sgr A*

Ponti et al. 2010
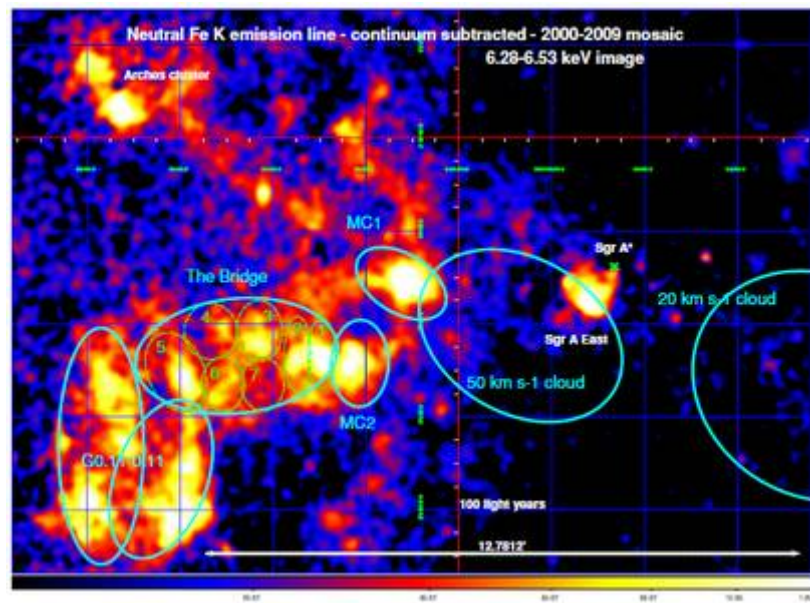
Clavel et al. 2013

- MCs are traced by line molecular emission like CS.
- MCs are not in circular motion => Position and velocity do not constrain the distance.
- MCs are identified by having similar velocity.

Time and space resolved of neutral Fe K line emission and continuum

Ponti et al., 2012 (XMM Fe K)
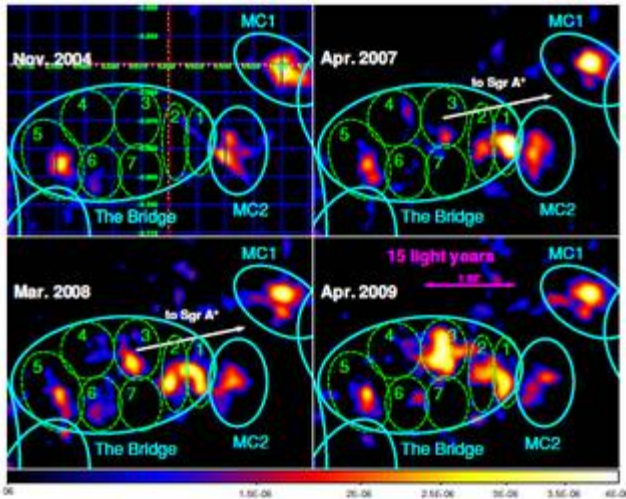
Clavel 2013, Chandra FeK
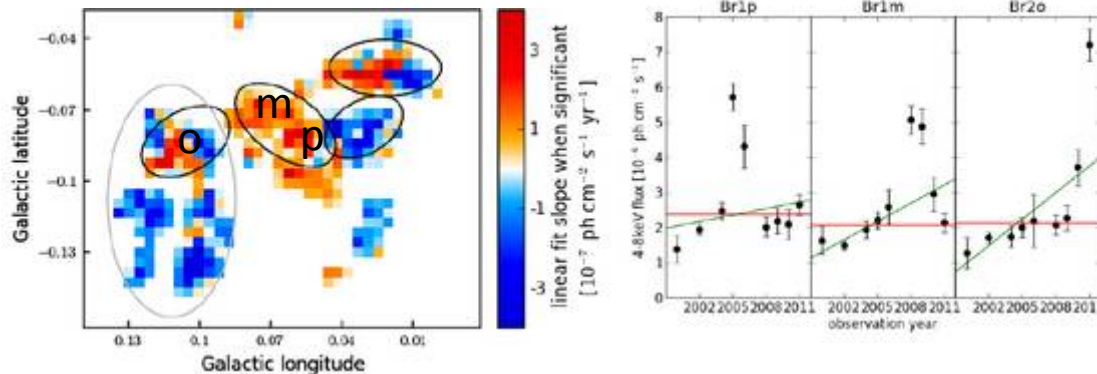
Clavel 2013, Chandra 4-8 keV trend.
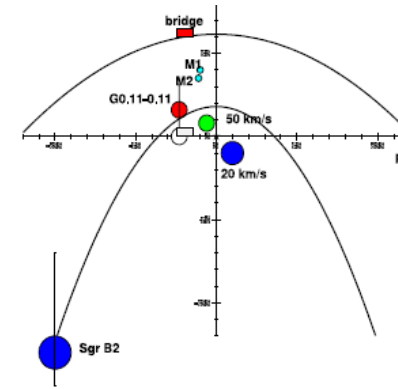
The position of the molecular clouds result from the hypothesis of a **single flare** seen by SgrB2 and G0.11-0.11, and the same luminosity of SgrA* as seen by the Bridge, MC1 and MC2.
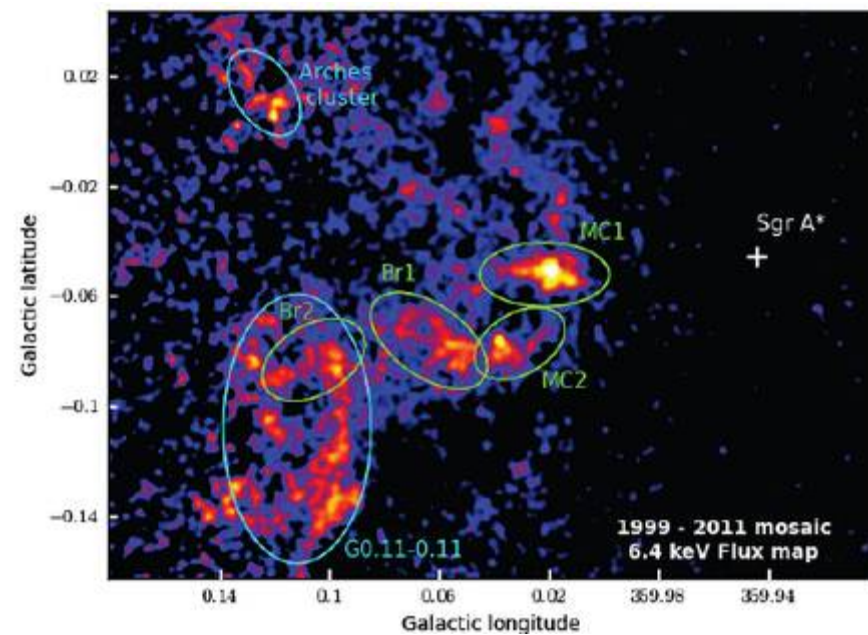
The single flare hypothesis is questioned by the 2 year event for the Bridge and 10 years trend from the other clouds :
two flares for Sgr A* ?

The time behavior of the cloud emission is indeed the convolution of their structure, their positions and the illuminating light-curve.

Fluxes from :

=> **'Sgr B2' -> Sidoli 2001, BeppoSAX, Continuum + Fe Line, 2-10 keV**

'Sgr B2 continuum' -> Murakami 2000, ASCA, Continuum Emission, 4-10 keV

=> **'Sgr C continuum' -> Murakami 2001, ASCA, Continuum Emission, 2-10 keV**

$\Rightarrow$ **'Sgr B2 - Hard' -> Terrier et al. (2010) ApJ 719:143 rescaled in the MEP band**

$\Rightarrow$ Ponti 2013:

- **G0.11-0.11**
- **Bridge**
- **M1**
- **M2**

Extended formula of the MDP

$$MDP = \frac{4.29}{\int \mu(E) \times A(E) \times \varepsilon(E) \times F(E) dE} \times \sqrt{\frac{\int (A(E) \times \varepsilon(E) \times F(E) + \int (B_{diff}(E) + B_{res}(E))) dE}{T}}$$
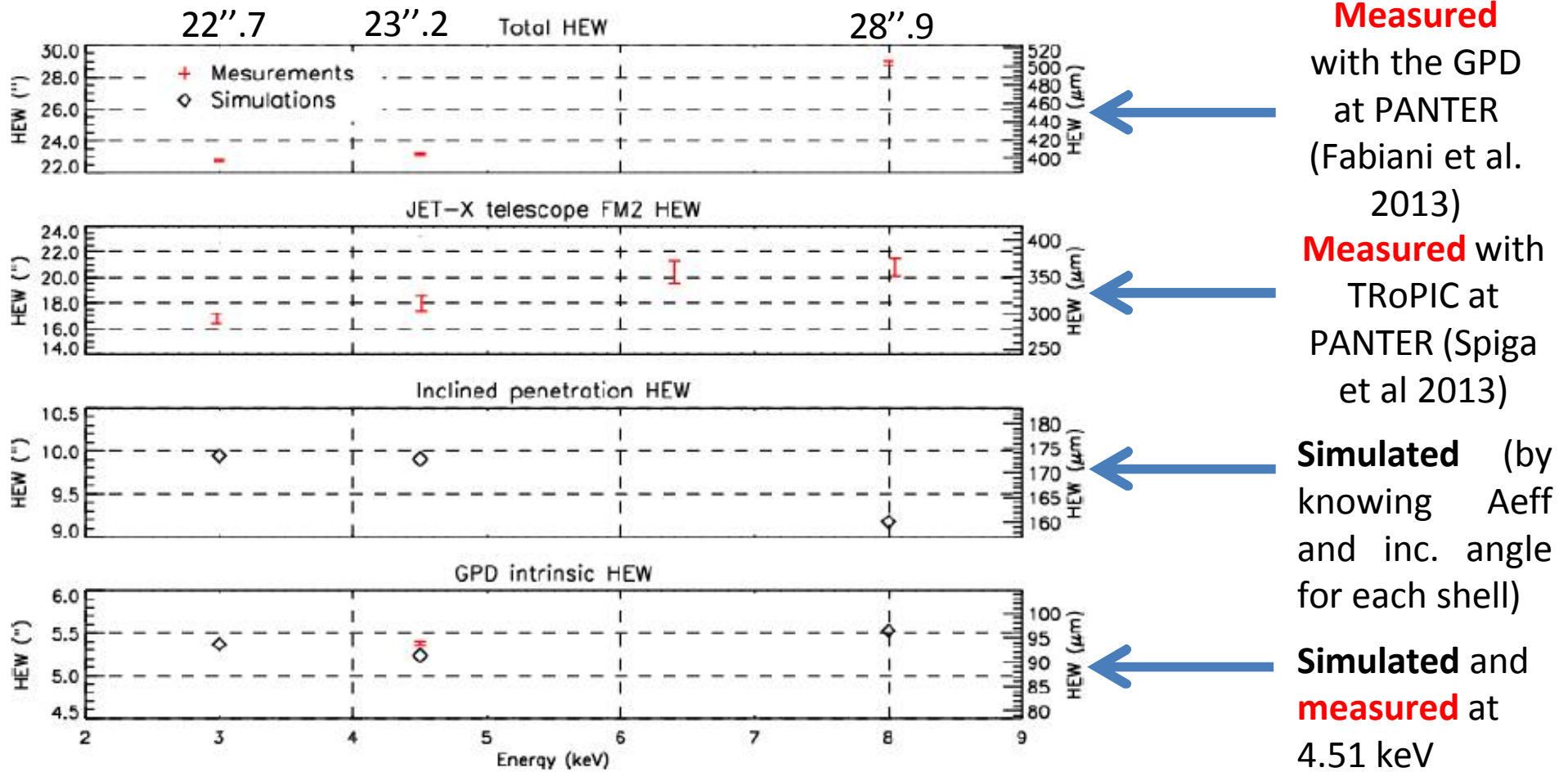
2.2 At the position of the best focus position we measured the Half Energy Width (HEW) at the three chosen energies and we compared the results with that obtained by distinguishing the three contribution :

Measured with the GPD at PANTER (Fabiani et al. 2013)

Measured with TRoPIC at PANTER (Spiga et al 2013)

Simulated (by knowing Aeff and inc. angle for each shell)

Simulated and **measured** at 4.51 keV
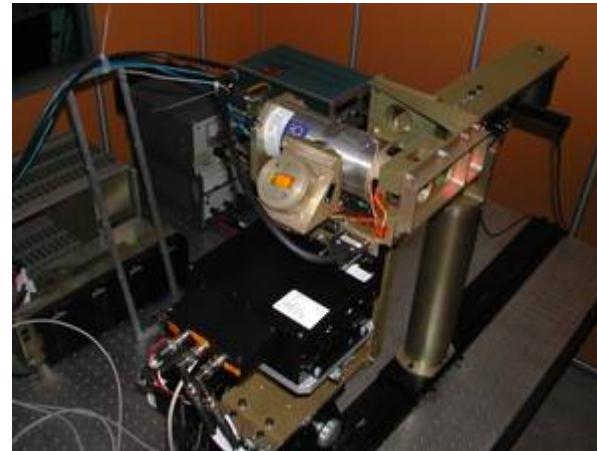
The results of the analysis show that the contribution to the total HEW are of decreasing importance going from the top to the bottom

Congresso Nazionale della SIF. Sezione Astrofisica

IASF-Rome facility for the production of polarized X-rays.

Facility at IASF-Rome/INAF

Close-up view of the polarizer and the Gas Pixel Detector

| keV	Crystal	Line	Bragg angle
1.65	ADP(101)	CONT	45.0
2.01	PET(002)	CONT	45.0
2.29	Rh(001)	Mo L_α	45.3
2.61	Graphite	CONT	45.0
3.7	Al(111)	Ca K_α	45.9
4.5	CaF_2(220)	Ti K_α	45.4
5.9	LiF(002)	^{55}Fe	47.6
8.05	Ge(333)	Cu K_α	45.0
9.7	FLi(420)	Au L_α	45.1
17.4	Fli(800)	Mo K_α	44.8

Capillary plate (3 cm diameter)

PET
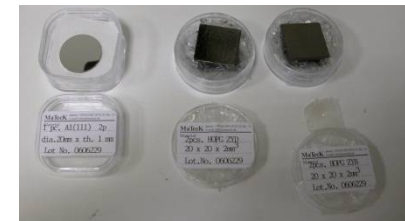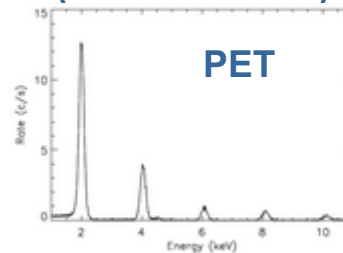
Aluminum and Graphite crystals.

Spectrum of the orders of diffraction from the Ti X-ray tube and a PET crystal acquired with a Si-PiN detector by Amptek

(Muleri et al., SPIE, 2008)

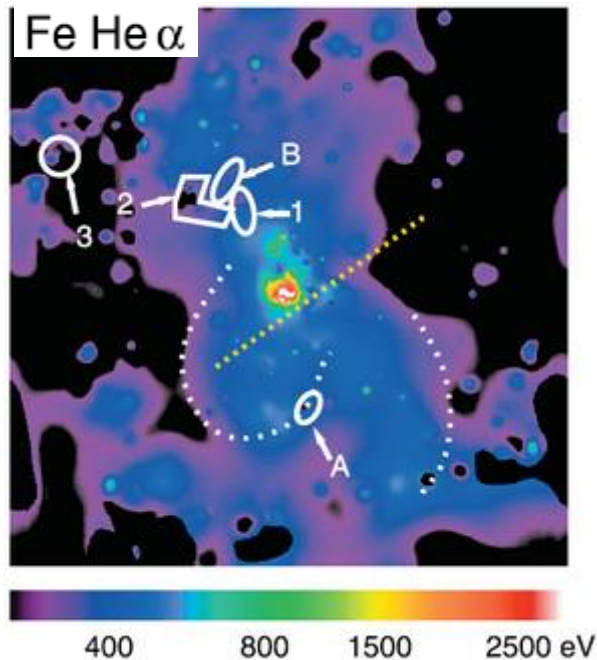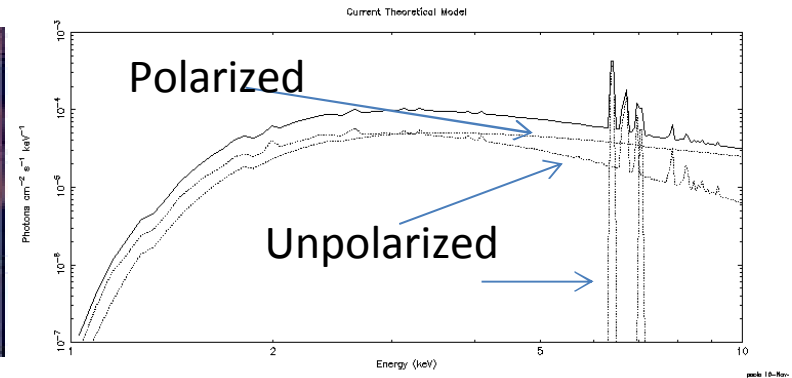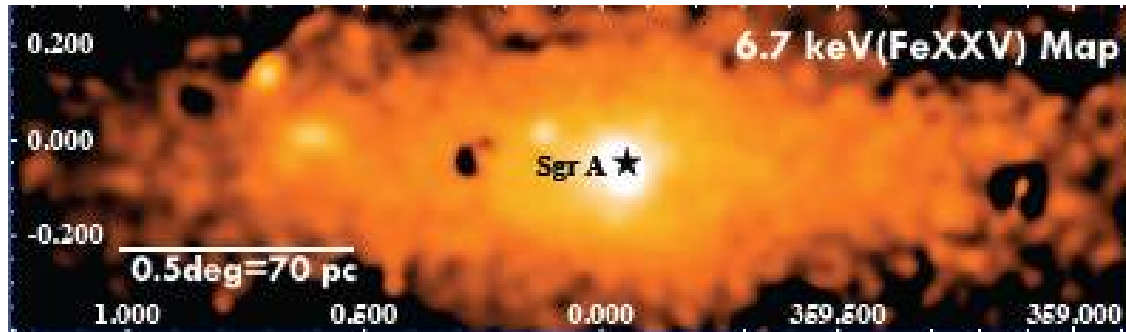The precision with which the measurement of the angle of polarization pinpoints the source of the primary emission.
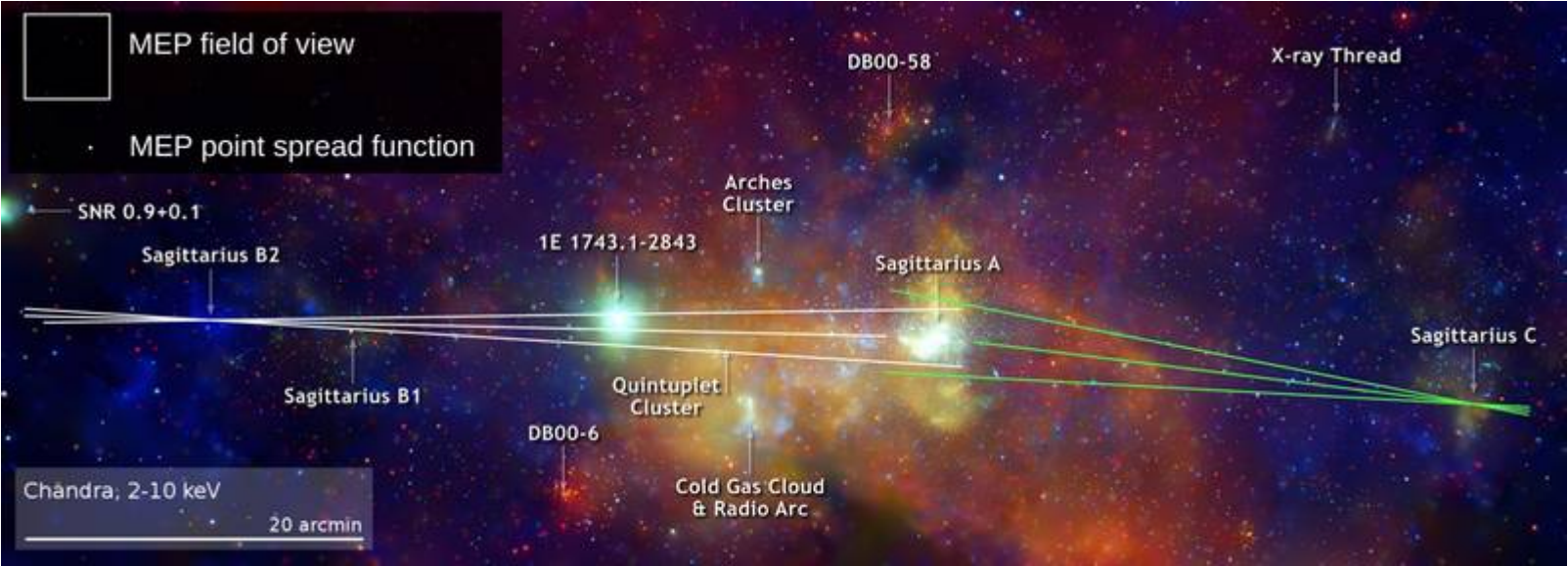
Constraints on the direction of the primary emission source with polarimetry on-board NHXM (500 ks of observation).

Source	P (Assumed)	Error on Angle
Sgr B2	20 %	2.2°
Sgr C	20 %	4.0°

Congresso Nazionale della SIF. Sezione Astrofisica

Not so easy in 2-10 keV

Map labels: 0.200, 0.000, -0.200; 6.7 keV(FeXXV) Map; Sgr A★; 0.5deg=70 pc; 1.000, 0.500, 0.000, 359.500, 359.000

Current Theoretical Model
Polarized
Unpolarized
Photons cm⁻² s⁻¹ keV⁻¹ ; Energy (keV)

Fe He α ; B ; 2 ; 1 ; 3 ; A ; 400 800 1500 2500 eV

- A diffuse emission typical of a hot plasma (6.5 keV) is present in the Galactic center region possibly providing not polarized component.

- The expected polarization due to reflection must be diluted considering this contribution to be estimated in different regions may be using the ionized Fe line strength.

- The not polarized fluorescence lines should be also taken into account when measuring polarization in a large energy range (2-10) .

Time and space resolved of neutral Fe K line emission with XMM

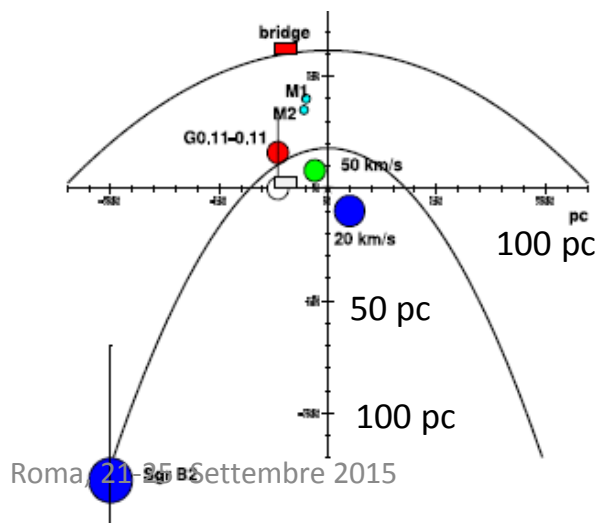XMM Space and time resolved spectroscopy (Fe K)
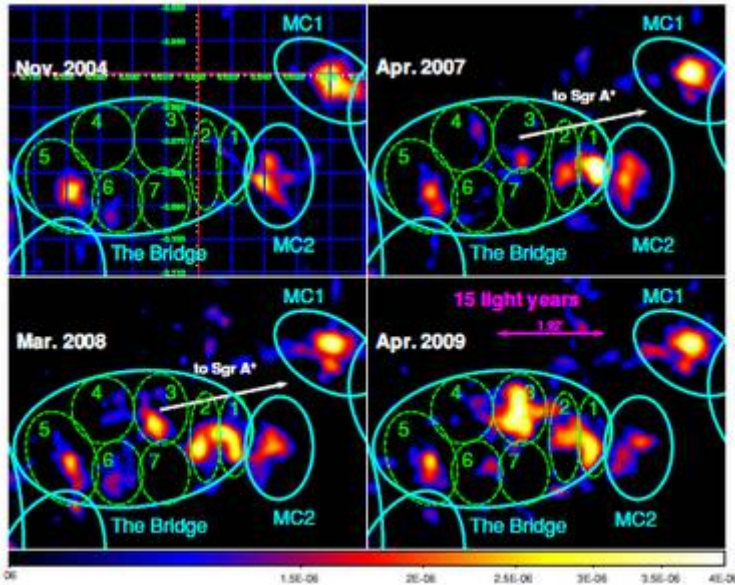
Ponti et al., 2012

- Apparent superluminal propagation west to east appears in XMM data of the bridge.
- Constant emission from MC1 and MC2.

The position of the molecular clouds result from the hypothesis of a **single flare** seen by SgrB2 and G0.11-0.11, and the same luminosity of SgrA* as seen by the Bridge, MC1 and MC2.


- Sketch of the positions of the molecular clouds as seen face on with SgrA* as black star on the vertex.

- The position of Sgr B2 is measured by parallax (Reid 2009.

- **SINGLE FLARE** The parabola connecting G0.11-0.11 and SgR B2 is the light front emitted 100 years ago. The further parabola represent a light front emitted 400 years ago.
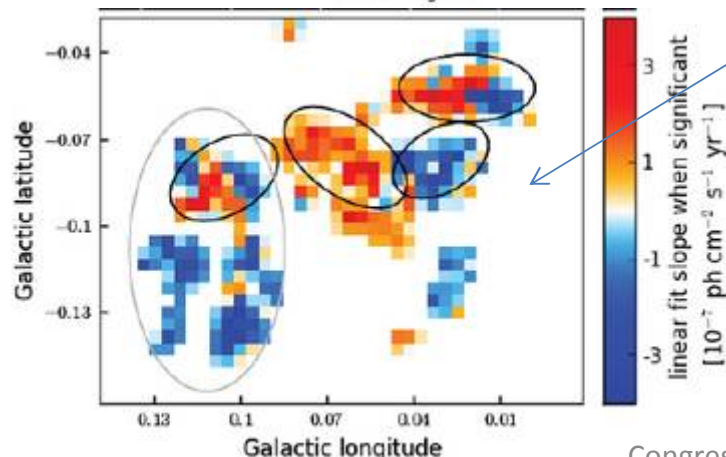
Time and space resolved of neutral Fe K line emission and continuum emission. Chandra

Clavel et al. 2013
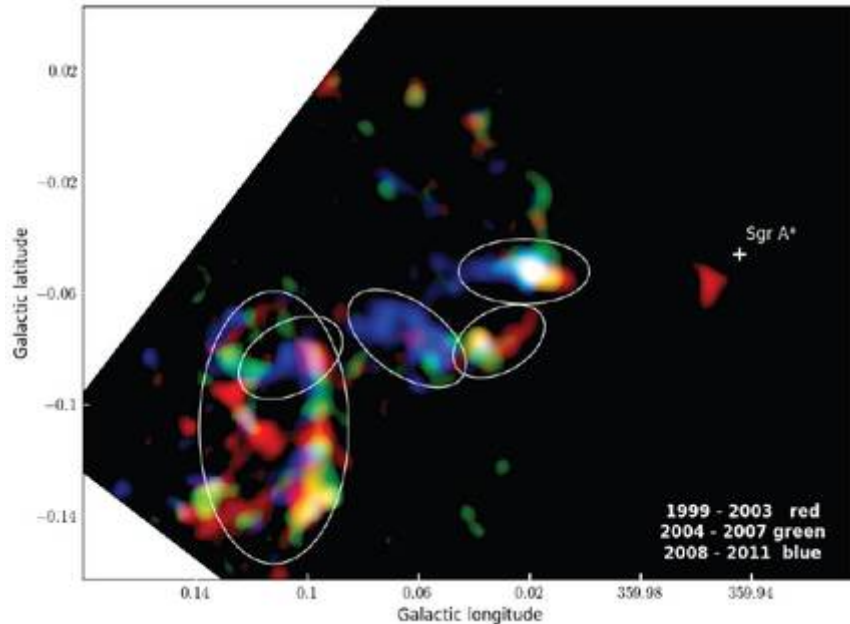
- Fe K line smoothed at 9 arcsec.

- Stongly varying emission in the Sgr A complex with a clear trend from west to east in MC1 and MC2 a late illumination in BR1 and BR2 and a more complex variation in G0.11-0.11.

4-8 keV linear fit slope of the light-curve.

- **Double flares.** Two illumination event would produce the observation pattern.

The time behavior of the clouds emission is the convolution of their structure, their positions and the illuminating light-curve.